Recognition of Surfaces Based on Haptic Information

Tomohiro Nakano

LUND
UNIVERSITY

Department of Automatic Control

MSc Thesis
ISRN LUTFD2/TFRT--5957--SE
ISSN 0280-5316

Department of Automatic Control
Lund University
Box 118
SE-221 00 LUND
Sweden

Printed in Sweden by Media-Tryck
Lund 2014

Abstract

The main topic and focus in this thesis are surface recognition.

In the sensing part, the surface information is collected as feature values. There are research approaches which focus on sensing surface tactile information by using sensors with robots. However, there are some disadvantages of using sensors. From that reason, this thesis proposes getting haptic surface information without sensors at the tip of robots. To this purpose, a disturbance observer is implemented to achieve the robust acceleration control and a reaction force observer is implemented to estimate the friction force along surfaces.

In the recognition part, a pattern recognition method needs to be applied for surface recognition. There are some pattern recognition methods, where self-organizing maps (SOM) is one of the solutions and has been investigated. SOM is able to summarize high-dimensional data to low dimension with preserving the topological properties of data. SOM is also suitable for multi-class recognition. Therefore, a surface recognition using SOM is proposed in this thesis. Multi-class surface recognition is achieved by the proposed method.

The validity of the proposed method was confirmed through 7 surface recognition experiments. The recognition rate was over 90% for 5 of 7 surfaces in the time domain.

Acknowledgements

I would like to express my gratitude to all the people who helped me with my research from a number of aspects. The results would have never been obtained without the help and support of many people.

I am deeply grateful to my examiner Professor Rolf Johansson. His enormous support and insightful comments were invaluable and always to the point which helped me pursuing my research. In addition, he gave me opportunities to do master thesis project and the summer job in the robotics laboratory. The experiences in robotics laboratory were valuable and gained my insights toward the theme.

I am also grateful to my advisor Professor Anders Robertsson. He gave me a lot of constructive and helpful advices although he was very busy. His supports have greatly contributed for my thesis. In addition, his smile always makes me happy to do work in the robotics laboratory.

I would like to give thanks to the members of robotics laboratory, advisor Mahdi Ghazaei, Fredrik Bagge Carlson and Adam Nilsson. I could not speak Swedish but they always talked to me in English. Therefore, I enjoyed the time in robotics laboratory and fika time of the Department of Automatic Control. I hope Mahdi and Fredrik will have a good time in Lund and that Adam will have a nice career in the USA.

My heartfelt appreciation goes to all of the members who I met in Sweden. For instance, members of master of wireless communication, members of Japanese studies in Lund University and so on. I would like to express my gratitude to Fumiaki Nagase and Hatto Mao.

Finally, I have a special note of thanks to my parents. They have supported me the whole of my period of studying abroad in Sweden. They encouraged me to go to Sweden for studying. Without their support, I could not complete my research for master course.

Contents

1. Introduction **9**
- 1.1 Background . . . 9
- 1.2 Problem Formulation . . . 10
- 1.3 Outline of this Research . . . 11

2. Methods **13**
- 2.1 Motion Control . . . 13
- 2.2 Haptic Information Acquisition . . . 19
- 2.3 Self-organizing Map (SOM) . . . 22

3. Experiments **25**
- 3.1 Experimental Setup . . . 25
- 3.2 Haptic Information Acquisition . . . 26
- 3.3 Surface Recognition by SOM . . . 27

4. Results **29**
- 4.1 Analysis of roughness and friction force . . . 29
- 4.2 Haptic Information Acquisition . . . 31
- 4.3 Surface Recognition by SOM . . . 33

5. Discussion **38**
- 5.1 Analysis of roughness and friction force . . . 38
- 5.2 Haptic Information Acquisition . . . 38
- 5.3 Surface Recognition by SOM . . . 39

6. Conclusion **40**

Bibliography **41**

1

Introduction

1.1 Background

"Real World Haptics" has received considerable attention in recent years. Real world haptics includes transmitting, recording and reproducing the information of the real environment [Zeng et al., 2013]. Example applications of haptics are surgery, medical training, micro manipulation and education. Haptics is an important technology for human assist field [Motooka et al., 2010] [Ferre et al., 2011] [From et al., 2014]. The technology to handle visual and audio information is established. However, real world haptics is a challenging theme because haptic information has bidirectionality. Haptic sensation mainly includes two kinds of information, force sensation and tactile sensation. In this paper, force sensation is defined as hardness or softness of the environment with the push-pull motion. Tactile sensation is defined as slippery or gritty of the environment at rubbing motion. In this paper, tactile sensation is focused on because it is important for humans to distinguish surfaces. For example, people slide their fingers to check the cloth texture in shopping. People change their grip force through surface roughness of objects. Therefore, it is clearly essential for robots to have an ability to recognize surfaces. Surface recognition is divided into two parts: the sensing part and the recognition part.

In the sensing part, there are some research approaches which focus on sensing of surface tactile information by using sensors with robots. Hosoda et al. used strain gauges and polyvinylidene fluoride (PVDF) films for robot fingers [Hosoda and Asada, 2006]. This finger could discriminate five different materials by pushing and rubbing the objects. Boissieu et al. used three-axial MEMS-based force sensors for the robot finger to analyse texture properties while sliding on surfaces [Boissieu et al., 2009]. This finger discriminated textures of 10 kinds of surfaces. Romano et al. used accelerometers to record and reproduce tactile sensations [Romano and Kuchenbecker, 2012]. These researchers achieved surface recognition by using sensors.

In the recognition part, there are some pattern recognition methods [Jain et al., 2000]. Pattern recognition methods are divided into two main groups, parametric

and non-parametric methods. Parametric methods such as Bayesian decision theory assume probability distribution of feature values. The disadvantage of parametric methods is that if the distribution of features is not known, parameters of the distribution must be estimated. On the other hand, non-parametric methods make no assumptions regarding the distributions of feature values. Therefore, non-parametric methods are suitable for using real world data sets. There are some parametric methods. Nozaki et al. recognized grasping motion using dynamic programming (DP) pattern matching algorithm [Nozaki et al., 2013]. DP matching is suitable for the recognition which has to take into account time warping. However, in the surface recognition, time warping is not necessary. Watabe et al. recognized and classified road conditions based on friction force information using support vector machine (SVM) [Watabe and Katsura, 2011]. Two classes of road conditions were recognized by online experiments. Jivko et al. recognized and categorized surfaces based on acceleration information using k-nearest neighbor algorithm (k-NN) and SVM [Sinapov et al., 2011]. Twenty different surfaces were recognized by offline experiments.

1.2 Problem Formulation

In the sensing part, previous research approaches achieved surface recognition by using sensors but there are some disadvantages [Katsura et al., 2007]. For example, an external force may be detected only at the position where the sensors are implemented. The cost of sensors may be one problem. Signal noise is also a problem since some force sensors detect an external force by amplifying a strain of the strain gauges, and then signal noise is also amplified.

Therefore, in the sensing part, this paper proposes getting haptic information of surfaces without sensors at the tip of multi degrees of freedom (DOF) robots. A disturbance observer (DOB) is implemented to achieve the robust acceleration control and to extract roughness information of surfaces [Ohnishi et al., 1996]. A reaction force observer (RFOB) is implemented to estimate friction force from surfaces in wide-band [Murakami et al., 1993]. Haptic information is acquired without sensors at the tip of the robots by applying DOB and RFOB. Some researchers used DOB and RFOB for haptic sensing without sensors [Mizoguchi et al., 2014] [Nozaki et al., 2014]. However, DOB and RFOB were applied to 1DOF or 2DOF robots. From a practical point of view, robots should have multi DOF. Therefore, in this paper, a multi DOF robot is used and haptic information of surfaces is acquired by DOB and RFOB without using force sensors.

In the recognition part, previous research approaches used k-NN and SVM for the surface recognition. k-NN and SVM are strong solutions for surface recognition. However, the computational effort is increased exponentially as the dimension of the feature vectors and number of class increases. This is a problem for online surface recognition by robots because longer sampling time deteriorates the control

Table 1.1 Symbols and indices used in this paper.

Symbol	Description	Index	Description
X	Position vector	*cmd*	Command
F	Force vector	*ref*	Reference
P	Feature vector	*res*	Response
K_p, K_v, K_f	Feedback gain	*n*	Number of elements
S^2	Sample variance	*rough*	Roughness
λ	Wavelength	*fric*	Friction

performance.

Therefore, in the recognition part, a surface recognition using self-organizing map (SOM) by a haptic robot is proposed. SOM was investigated by Kohonen in the early 1980s [Kohonen, 2001]. SOM was applied to a wide field of problems. For instance, document plagiarism detection [Chow and Rahman, 2009], object detection in surveillance systems [Chacon-Murguia and Gonzalez-Duarte, 2012] and superquadric-based model of the human motion [Najmaei and Kermani, 2011]. SOM is one of the neural network architecture that is trained using unsupervised learning [Brugger et al., 2008]. SOM is able to summarize high dimensional data to low dimension with preserving the topological properties of data. Therefore, non-linear data summarization is possible and it is suitable for multi-class recognition. Another characteristics of SOM are data visualization and simple algorithm. Chen et al. showed that SVM and SOM have almost the same performance for offline classification simulations [Chen et al., 2006]. SOM is chosen in this paper from the computational effort point of view for online surface recognition. Therefore, many classes of surfaces can be recognized by multiple feature values.

1.3 Outline of this Research

An outline of the proposed method is shown in Figure 1.1. Symbols and indices used in this paper are shown in Table 1.1.

In the training part, a SOM model is generated from training data. In this paper, feature values are extracted from haptic information. Haptic information is defined as position information and force information. Both measurements are acquired by the haptic robot which any sensors are not attached at the tip. In this paper, Omega 7 from Force Dimension is used as haptic robot. After the feature values are extracted, The SOM model is generated.

In the test part, feature values are extracted by the same way as training part. Recognition is conducted by comparing SOM model, which is generated in the training part, and feature values from the test data.

The validity of the proposed surface recognition method was verified by experiments with actual environmental surfaces.

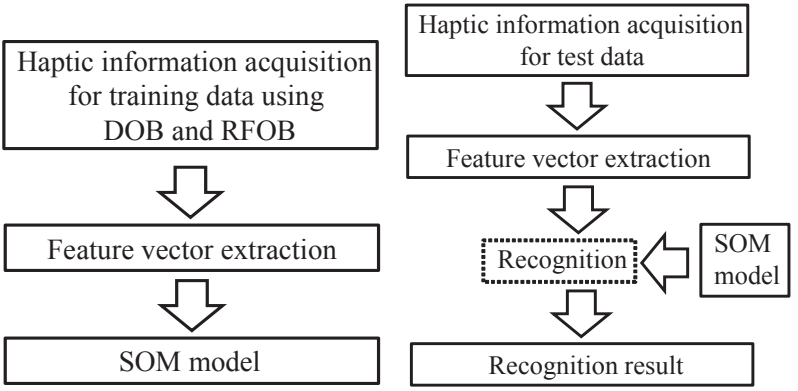

(a) Training (b) Test

Figure 1.1 Outline of the proposed method.

2

Methods

In this chapter, methods used in this research are explained. First, motion control, which is essential to achieve reaction force estimation without force sensors, is explained. After that, the haptic information acquisition system is introduced to calculate feature values of surfaces. Finally, self-organizing maps. which is used for surface recognition is explained.

2.1 Motion Control

This section describes acceleration-based control method for robots. In addition, reaction force estimation method is explained. For ease of the modeling, it is assumed that robots mentioned in this chapter are actuated by 1-DOF linear motor. The linear motor is modeled in Section 2.1. After that, acceleration-based control using DOB is explained in Section 2.1. Then in Section 2.1, reaction force estimation method using RFOB is introduced.

Modeling

Defining the linear motor position as x, mass as M, driving force as f^m and load force as f^{load}, the motion equation of the linear motor is written as Eq. (2.1).

$$M\ddot{x} = f^m - f^{load} \tag{2.1}$$

The driving force f^m is expressed as Eq. (2.2).

$$f^m = K_t I_a^{ref} \tag{2.2}$$

I_a^{ref} and K_t are armature current reference and thrust torque constant. The load force is defined as Eq. (2.3) in this paper.

$$f^{load} = f^{ext} + f^g + f^{fric} \tag{2.3}$$

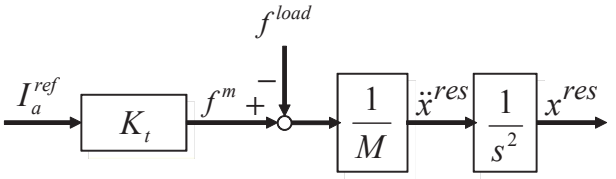

Figure 2.1 Dynamics of linear motor.

f^{ext} is the external force, f^g is gravitational force and f^{fric} is the frictional force which consists of static and viscous frictions. From Eqs. (2.2) and (2.3), the motion equation can be rewritten as Eq. (2.4).

$$M\ddot{x} = K_t I_a^{ref} - (f^{ext} + f^g + f^{fric}) \tag{2.4}$$

The mass M and the thrust torque constant K_t vary according to the posture of the robot or magnetic flux distribution. M and K_t, which considering parameter perturbations, can be written as Eqs. (2.5) and (2.6).

$$M = M_n + \Delta M \tag{2.5}$$

$$K_t = K_{tn} + \Delta K_t \tag{2.6}$$

Here, subscript n denotes the nominal values of parameters. By substituting Eqs. (2.5) and (2.6) to Eq. (2.4), the motion equation can be expressed as Eq. (2.7).

$$M_n\ddot{x} \quad = \quad K_{tn} I_a^{ref} - (\Delta M\ddot{x} - \Delta K_t I_a^{ref} + f^{load}) \tag{2.7}$$

In this paper, disturbance is defined as Eq. (2.8).

$$f^{dis} = f^{load} + \Delta M\ddot{x} - \Delta K_t I_a^{ref} \tag{2.8}$$

The block diagram of the linear motor is shown in Figure 2.1.

Acceleration based control using disturbance observer

In this subsection, acceleration-based control using disturbance observer is described.

The second-order derivative of position is acceleration. In addition, acceleration is also derived by dividing force by mass. From these reasons, position and force can be controlled by controlling acceleration. Furthermore, position and force are controlled robustly by acceleration control with disturbance observer (DOB)[Ohnishi et al., 1996].

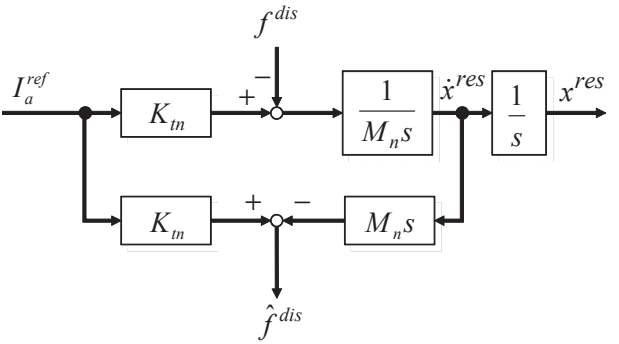

Figure 2.2 Block diagram of DOB.

Disturbance observer DOB is one of the observer which estimates a disturbance from input and output information. In other word, DOB is one the method to achieve robust control. The block diagram of DOB is shown in Figure 2.2.

The disturbance applied to the linear motor is written as Eq. (2.9) from Eq. (2.7).

$$f^{dis} = K_{tn} I_a^{ref} - M_n \ddot{x}^{res} \tag{2.9}$$

From Eq. (2.9), the disturbance can be calculated from the current reference I_a^{ref} and the acceleration response $\ddot{x}^{res}$. In this paper, acceleration response is obtained by measurements from a position encoder. Therefore, the effect of noise is magnified and the estimated acceleration is deteriorated by second-order differentiation. In this paper, a low-pass filter (LPF) is applied to eliminate the effect of the noise. The estimated disturbance is written as Eq. (2.10). A first-order LPF is used in this paper written as Eq. (2.11).

$$\hat{f}^{dis} = G_{lpf}(s) f^{dis} \tag{2.10}$$

$$G_{lpf}(s) = \frac{g_{dis}}{s + g_{dis}} \tag{2.11}$$

g_{dis} is the cut-off frequency of the DOB.

The block diagram of the actual DOB is shown in Figure 2.3. In Figure 2.3, there is a differentiation of the velocity. Therefore, pseudo differentiation is implemented to eliminate the effect of high frequency noise. The block diagram can be equivalently modified as Figure 2.4.

The compensation current I^{cmp} is calculated as Eq. (2.12).

$$I^{cmp} = \frac{1}{K_{tn}} \hat{f}^{dis} \tag{2.12}$$

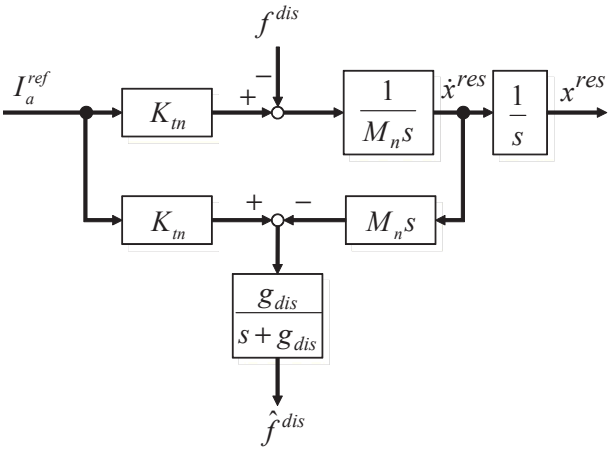

Figure 2.3 Block diagram of actual DOB.

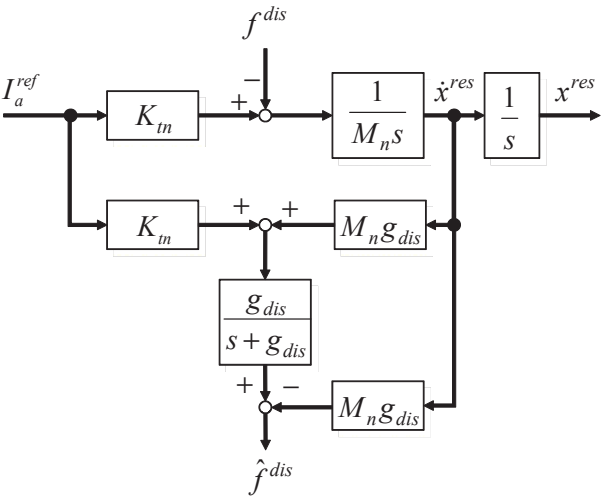

Figure 2.4 Block diagram of equivalently modified DOB.

Robust control is achieved by feedback compensation current I^{cmp} to the input current. The block diagram of the disturbance compensation by DOB is shown in Figure 2.5.

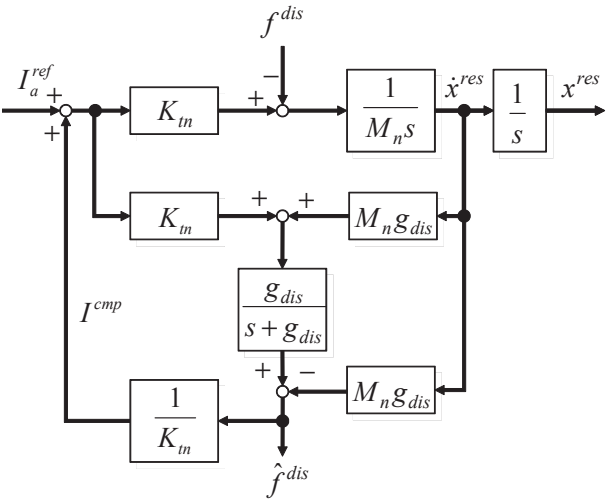

Figure 2.5 Block diagram of disturbance compensation by DOB.

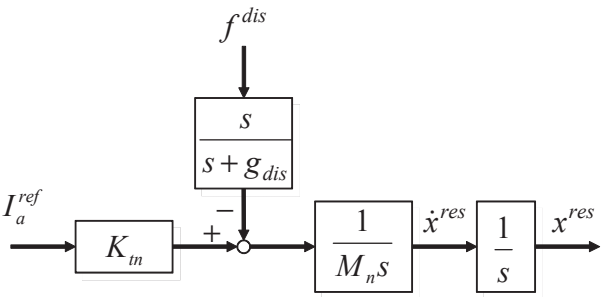

Figure 2.6 Block diagram of equivalently modified DOB shown in Figure 2.5.

Acceleration controller Figure 2.5 can be equivalently modified to Figure 2.6. Figure 2.6 indicates that the disturbance passes through a high-pass filter (HPF) and then affects the system. The HPF is written as Eq. (2.13).

$$G_{hpf}(s) = \frac{s}{s+g_{dis}} \tag{2.13}$$

$G_{hpf}(s)$ is called sensitivity function since Eq. (2.13) indicates a sensitivity to the disturbance toward the system. The low-frequency disturbance is suppressed. On the other hand, the high-frequency disturbance is not eliminated and affects the

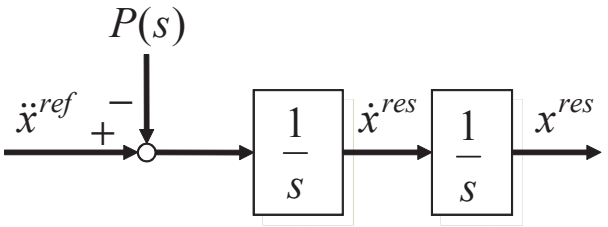

Figure 2.7 Block diagram of DOB using acceleration disturbance.

system. For these reasons, the high cut-off frequency of the DOB, g_{dis}, provides a small sensitivity function and provides the wide bandwidth for robust motion control. However, too high cut-off frequency leads to instability of the system.

In Figure 2.6, the difference between reference and response of the acceleration is defined as $P(s)$ in this paper. $P(s)$ is called equivalent acceleration disturbance and expressed as Eq. (2.14).

$$\begin{aligned} P(s) &= \ddot{x}^{ref} - \ddot{x}^{res} \\ &= M_n^{-1} G_{hpf}(s) f^{dis} \end{aligned} \tag{2.14}$$

The block diagram of the DOB using $P(s)$ is shown in Figure 2.7. Input of the DOB is an acceleration reference from Figure 2.7. In conclusion, the robust control using DOB is the same as acceleration control which achieves desired acceleration reference since the input is the acceleration.

Reaction force observer

A reaction force observer (RFOB) is an observer which estimates the external force f^{ext} from the estimated disturbance f^{dis} by DOB. Force estimation without force sensors is possible by using RFOB.

The disturbance estimated by using DOB is written as Eq. (2.3) and Eq. (2.7). Therefore, external force can be derived as Eq. (2.15).

$$f^{ext} = f^{dis} - f^{g} - f^{fric} - \Delta M\ddot{x} + \Delta K_t I_a^{ref} \tag{2.15}$$

Equation (2.15) indicates that the external force can be estimated if the right-hand-side terms can be identified. In this paper, disturbance f^{dis} is estimated by DOB. The internal force f^{int} is assumed to be 0. In addition, parameter perturbations are assumed to be 0. Hence, in the sequel, we assume that the external force f^{ext} is written as Eq. (2.16).

$$f^{ext} = f^{dis} - f^{g} - f^{fric} \tag{2.16}$$

For multi-DOF robots with friction and gravity forces, the right-hand-side terms are pre-identified and subtracted from f^{dis} to estimate the external force as shown

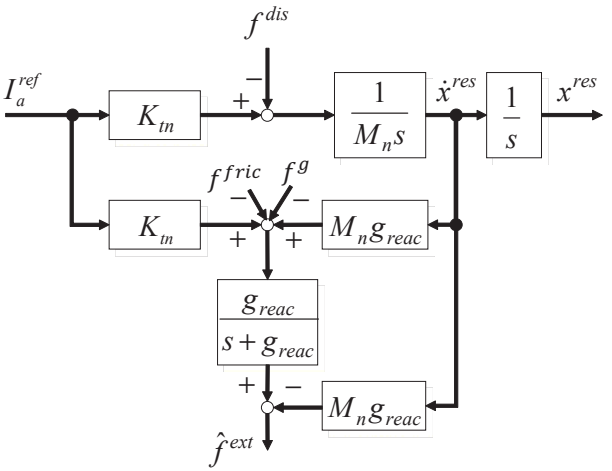

Figure 2.8 Block diagram of RFOB.

in Eq. (2.16). Since the external force is identified with noise similar to DOB, the external force is estimated through the LPF as Eq. (2.17).

$$\hat{f}^{ext} = \frac{g_{reac}}{s+g_{reac}} f^{ext} \tag{2.17}$$

The parameter g_{reac} is the cut-off frequency of the RFOB. The block diagram of the RFOB is shown in Figure 2.8. The reaction force is estimated from the current reference I_a^{ref} and the velocity output $\dot{x}^{res}$.

2.2 Haptic Information Acquisition

In this section, a haptic information acquisition system is introduced to get haptic information.

Figure 2.9 shows the surface sensing system in this thesis. The coordinate frame is also shown in Figure 2.9. The rubbing motion is conducted to the surfaces by the tip of the robot. The control systems of the robot and the feature value collection are explained in the rest of this section.

Control Systems

In this thesis, the position control was applied to the x-axis and the force control was applied to the z-axis for rubbing motion. That is because position outputs of the z-axis and reaction force outputs of the x-axis are needed to calculate feature values.

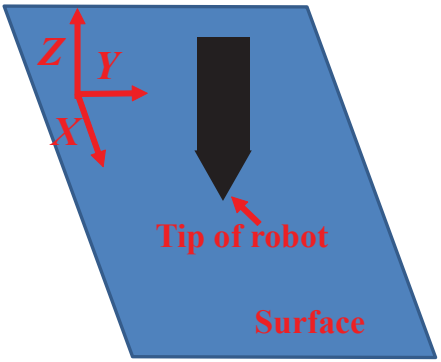

Figure 2.9 Surface sensing system.

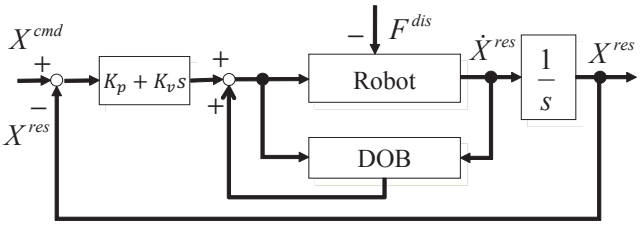

Figure 2.10 Block diagram of position control.

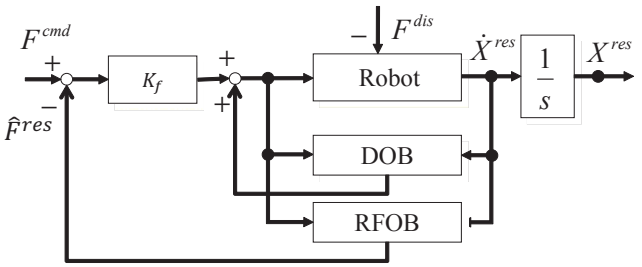

Figure 2.11 Block diagram of force control.

Block diagrams of position control and force control are shown in Figure 2.10 and Figure 2.11. DOB was used to achieve the robust acceleration control. RFOB was used to estimate reaction force from the environment.

Figure 2.12 shows the result of the force control experiment to prove the validity of the reaction force estimation. In this experiment, the tip pushed the force sensor directly. Mini 40 was used for the force sensor. From Figure 2.12, the maximum

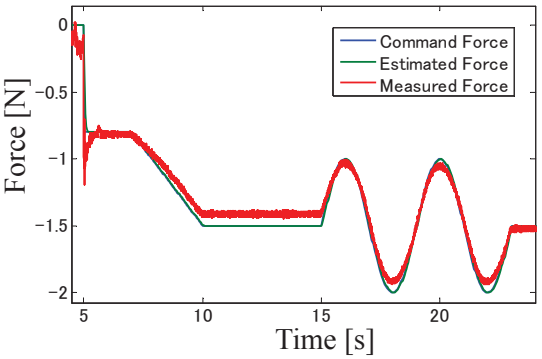

Figure 2.12 Force control experiment.

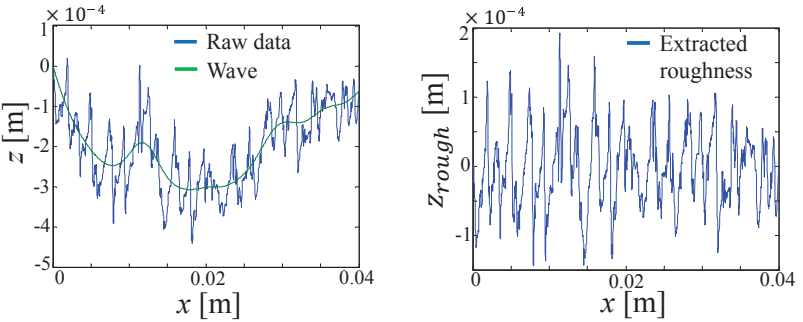

(a) Raw position data

(b) Extracted roughness

Figure 2.13 Roughness extraction.

error was about 0.1N. The reaction force estimation was achieved by using RFOB. Therefore, the validity of the reaction force estimation was verified. From these reasons, the reaction force of x-axis, which is same as the friction force of the suraface can be estimated accurately.

Feature Values Collection

Haptic information is acquired as feature values by the rubbing motion. Feature values are required for the surface recognition by self-organizing map (SOM). Rubbing motion is achieved by the position control for the x-axis and force control for the z-axis. Therefore, position data of the z-axis and reaction force data of the x-axis are valuable. In this thesis, the position data along the z-axis is defined as "Roughness"

and reaction force data along the x-axis is defined as "Friction".

Feature values from the roughness Raw position data include waviness component and roughness component. The roughness can be extracted by a high pass filter. The example of the raw position data and extracted roughness are shown in Figure 2.13. Average absolute $\overline{z_{rough}}$, sample variance S^2_{rough} and average wavelength $\overline{\lambda}$ of the roughness are extracted as feature values in this paper. Three feature values are derived as Eqs. (2.18), (2.19) and (2.20).

$$\overline{z_{rough}[n]} = \frac{1}{n}\sum_{i=1}^{n}|z_{rough}[i]| \tag{2.18}$$

$$S^2_{rough}[n] = \frac{1}{n}\sum_{i=1}^{n}(\overline{z_{rough}[n]} - z_{rough}[i])^2 \tag{2.19}$$

$$\overline{\lambda[n]} = \frac{x}{k} \tag{2.20}$$

n is the number of data. k is defined as number of the waves in this paper. Extracted roughness was approximated by zero phase low pass filter and the k was calculated by counting the number of approximated wave.

Feature values from the friction force Average friction $\overline{f_x}$ and sample variance of friction S^2_{fric} are extracted as feature values in this paper as Eqs. (2.21) and (2.22).

$$\overline{f_x[n]} = \frac{1}{n}\sum_{i=1}^{n}f_x[i] \tag{2.21}$$

$$S^2_{fric}[n] = \frac{1}{n}\sum_{i=1}^{n}(\overline{f_x[n]} - f_x[i])^2 \tag{2.22}$$

Feature vector From Section 2.2 and Section 2.2, the feature vector for SOM is written as Eqs. (2.23), (2.24) and (2.25).

$$\mathrm{P} = [\overline{\mathrm{z_{rough}}}\ \ \mathrm{S^2_{rough}}\ \ \overline{\lambda}\ \ \overline{\mathrm{f_x}}\ \ \mathrm{S^2_{fric}}]^{\mathrm{T}} \tag{2.23}$$

$$= [\mathrm{p_1}\ \ \mathrm{p_2}\ \ \cdots\ \ \mathrm{p_n}] \tag{2.24}$$

$$\mathrm{p_i} = [\overline{z_{rough}[i]}\ \ S^2_{rough}[i]\ \ \overline{\lambda[i]}\ \ \overline{f_x[i]}\ \ S^2_{fric}[i]]^{\mathrm{T}} \tag{2.25}$$

2.3 Self-organizing Map (SOM)

In this section, the self-organizing map (SOM) is explained. The SOM is a neural network architecture [Brugger et al., 2008]. SOM is able to summarize high dimensional data to low dimension with preserving the topological properties of data. The data are usually organized in 1D or 2D representations, so that data visualization is possible. In addition, SOM is able to represent the non-linear features, so it is suitable for multi-class clustering as compared with SVM.

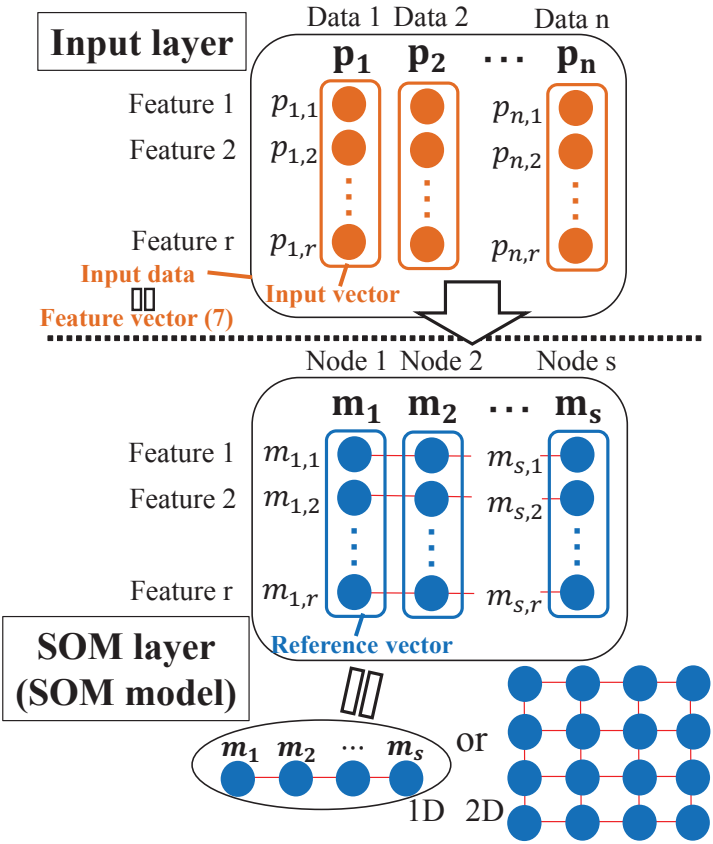

Figure 2.14 Architecture of SOM.

Architecture of SOM

The SOM architecture is shown in Figure 2.14. r is the dimension of the feature vector and s is the number of SOM nodes. SOM is composed of an input layer and SOM layer. The feature vector is used for the input layer. Nodes are arranged as one or two dimensions in the SOM layer. Each node has a reference vector which has the same dimensions r as the feature vector. A one-dimensional SOM is used and $r = 5$ in this paper.

Algorithm of SOM

The algorithm of SOM is explained in this subsection.

1. Dimension and number of nodes are decided.

2. Each feature value of the input data is normalized that the amplitude of each feature value becomes 1. For instance, feature value 1 in Figure 2.14 is normalized as Eq. (2.26).

$$p_{i,1} = \frac{p_{i,1}}{\sqrt{p_{1,1}^2 + p_{2,1}^2 + \cdots + p_{n,1}^2}} \tag{2.26}$$

3. Reference vector is generated randomly at each node of the SOM layer. After that, each reference vector is normalized that the amplitude of each reference vector becomes 1.

4. The i^{th} input vector is sent to SOM layer to make the SOM model. The inner product between the input vector and each reference vector is calculated. The node which has biggest inner product is chosen as the "winner" node. The winner node number of i^{th} input vector is defined as c_i in this paper. c_i is calculated as Eq. (2.27).

$$c_i = \arg \max(\mathrm{m_q} \cdot \mathrm{p_i}), (q = 1, \cdots, s) \tag{2.27}$$

5. The winner node and neighborhood nodes learn the input vector. Learning is achieved by a reinforcement function. Normal distribution is used for reinforcement function in this paper. Reinforcement function h_i is defined as Eq. (2.28).

$$h_i = \alpha \exp\left(-\frac{(r_i - r_{win})^2}{2\sigma^2}\right) \tag{2.28}$$

where α is called learning rate, α indicates the strength of learning, σ is the standard deviation of normal distribution, r_i is the position of the i^{th} node and r_{win} is the position of the winner node. SOM learning is achieved and the reference vector of the winner node is calculated by Eq. (2.29).

$$\mathrm{m_i} = \frac{\mathrm{m_i} + h_i \mathrm{p_i}}{||\mathrm{m_i} + h_i \mathrm{p_i}||} \tag{2.29}$$

6. Repeat steps 4) and 5) arbitrary times Z. The input vector is chosen randomly from the input data.

Parameters, which have to be set up, are as follows:

- Number of nodes s
- Learning rate α
- Standard deviation of reinforcement function σ
- Repeat counts of learning Z

3

Experiments

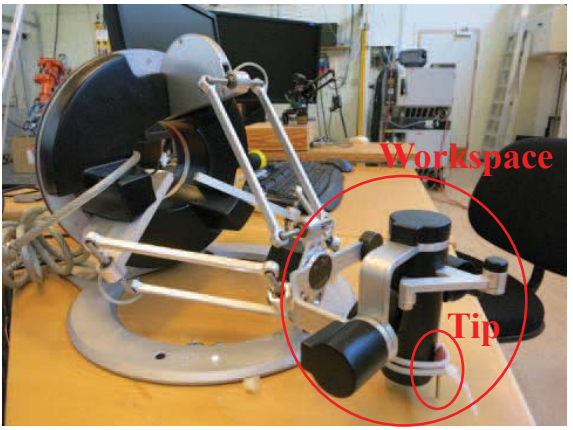

Figure 3.1 Robot (Omega7) used in the experiments.

In this chapter, surface recognition experiments are explained.

3.1 Experimental Setup

The robot used in this paper was an Omega 7 from Force Dimension [De Donno et al., 2013]. Omega 7 is a parallel haptic device with force feedback in three translational degrees of freedom and one degree of freedom in a pinching motion. Figure 3.1 shows the overview of the Omega 7. Figure 3.2 shows the tip of the Omega 7. The coordinate frame used in this paper is also shown in Figure 3.2. In this paper, the axis parallel to the surface was defined as x-axis and the axis perpendicular to the surface is defined as z-axis. A pen was attached at the tip. The rubbing motion was conducted by the pen. Surfaces which were used in the experiments are shown

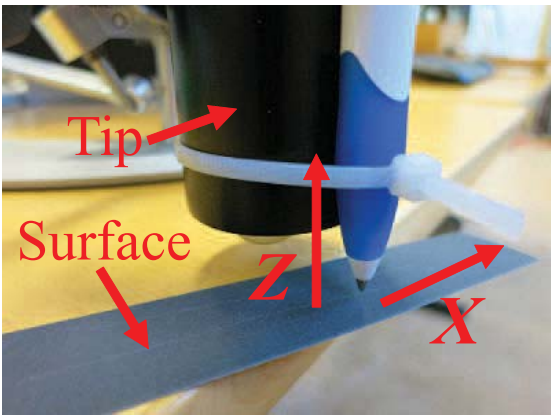

Figure 3.2 Tip of the robot.

(a) Sandpapers

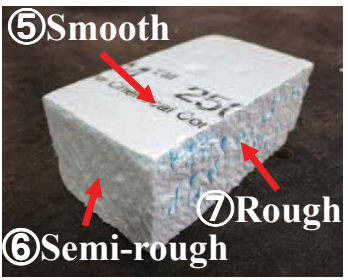

(b) Styrol

Figure 3.3 Surfaces used in the experiment.

in Figure 3.3. There were 4 kinds of sandpapers and 3 kinds of different surfaces of the styrol. The purpose of this paper is recognizing these 7 surfaces.

3.2 Haptic Information Acquisition

First of all, haptic information was acquired as feature values by the rubbing motion. Parameters and commands for rubbing motion experiments are shown in Table 3.1 and Table 3.2. Rubbing motion was conducted three times to each surface. One time for training and two times for recognition tests.

Table 3.1 Parameters for experiment.

Parameter	Description	Value
st	Sampling time	$0.3ms$
K_p	Position gain	900 s^{-2}
K_v	Velocity gain	60 s^{-1}
K_f	Force gain	0.8
g_{dis}	Cutoff frequency of DOB	50 rad/s
g_{reac}	Cutoff frequency of RFOB	50 rad/s
M_n	Nominal mass of workspace	0.3 kg

Table 3.2 Commands of rubbing motion

Symbol	Value
F_z^{cmd}	0.3 N
$\dot{x}_{cmd}$	0.005 m/s

Table 3.3 Parameters for SOM.

Parameter	Description	Value
s	Number of nodes	12
α	Learning rate	Eq. (3.1)
σ	Standard deviation of reinforcement function	1.6
Z	Repeat counts	10000

3.3 Surface Recognition by SOM

After the feature values are calculated, the surfaces shown in Figure 3.3 were recognized by SOM. Parameters for SOM in the training are shown in Table 3.3. A 1D SOM model was used in this paper. The parameters of SOM were decided by trial and error to achieve the higher recognition rate. Initial reference vectors of the SOM model were set randomly. The learning rate α is written as Eq. (3.1).

$$\alpha_i = 0.3 \cdot (1 - (i/Z)), \quad (i = 1, \cdots, Z) \tag{3.1}$$

α was decreased as the number of i was increased because the learning rate should be large at the beginning of the training due to the randomness of the initial reference vectors of the SOM model.

First of all, the SOM model was learned by using training data obtained in Section 3.2. The SOM algorithm was applied to the training data.

After that, surface recognition experiment was conducted to recognize surfaces by using the SOM model learned in the training. In this paper, surface recognition was conducted off-line in Matlab. However, the same recognition algorithm can be used for on-line experiment. Surface recognition was achieved by Eq. (2.27).

The inner product between the input vector from the test data and the reference vector from learned SOM model were calculated. The node which has biggest inner product was the winner node and surface was recognized. For example, if the winner node is 1, surface recognition result is a "smooth" surface.

4

Results

The results from the surface recognition experiments are shown and analyzed in this chapter.

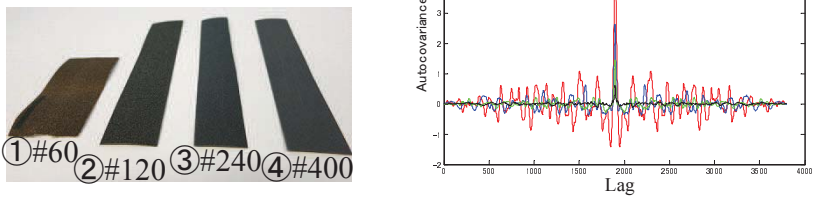

(a) Sandpapers (b) Autocovariance of roughness

Figure 4.1 Autocovariance of roughness (Sandpapers).

4.1 Analysis of roughness and friction force

In this paper, feature values are calculated from roughness and friction force. Therefore, analysis results of the roughness and friction force are shown in this section. Roughness and friction force were analyzed by autocovariance.

Autocovariance of the roughness

Figure 4.1 shows the autocovariance of the roughness of sandpapers. Figure 4.2 shows the zoomed one of Figure 4.1. Figure 4.2 focuses on the maximum value of the autocovariance and the distance between maxima. From Figure 4.2, the differences between surfaces can be found.

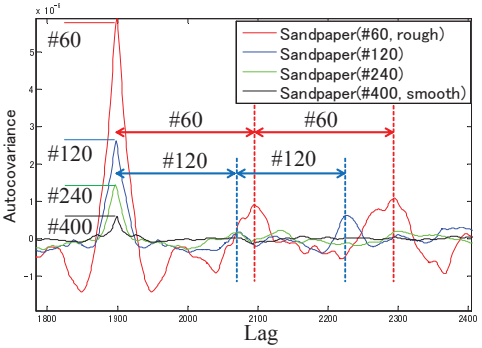

Figure 4.2 Zoomed autocovariance of roughness (Sandpapers).

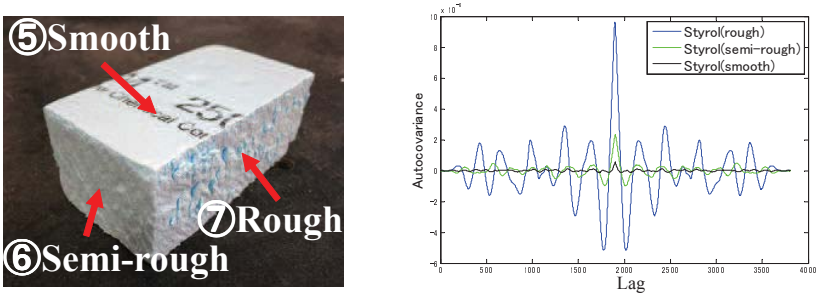

(a) Styrol (b) Autocovariance of roughness

Figure 4.3 Autocovariance of roughness (Styrol).

Figure 4.3 shows the autocovariance of the roughness of styrol surfaces. From Figure 4.3, it is obvious that there are differences of autocovariance between rough, semi-rough and smooth styrol surfaces.

Figure 4.4 shows the autocovariance of the roughness of sandpapers and styrol surfaces. Figure 4.5 shows the zoomed one of Figure 4.4. In Figure 4.5, sandpaper #120 and semi-rough styrol surfaces have similar maximum autocovariances. However, the distances between maxima are different.

Autocovariance of the friction force

Figure 4.6 shows the autocovariance of the friction of sandpapers. Figure 4.7 shows the zoomed one of Figure 4.6. From Figure 4.7, each surface has a different maximum autocovariance. However, it is hard to find the differences of the distance between maxima.

Figure 4.8 shows the autocovariance of the friction of styrol surfaces. From

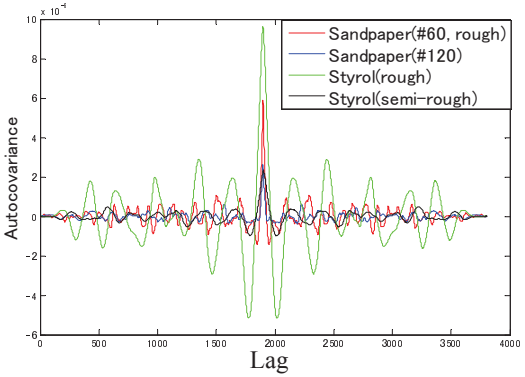

Figure 4.4 Autocovariance of roughness (Sandpaper and styrol).

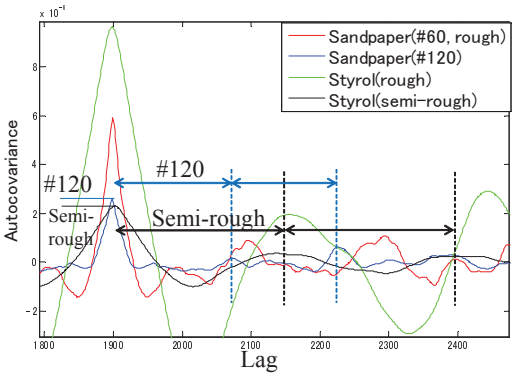

Figure 4.5 Zoomed autocovariance of roughness (Sandpaper and styrol).

Figure 4.8, each surface has different autocovariance. In addition, each surface has different distance between maxima.

4.2 Haptic Information Acquisition

Roughness and friction force are the important parameters to recognize surfaces from the results of Section 4.1. Feature values which are used in the surface recognition are calculated from roughness and friction force. Calculated feature values are shown in this section.

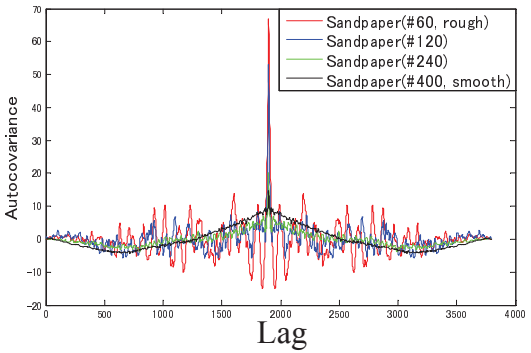

Figure 4.6 Autocovariance of friction (Sandpaper).

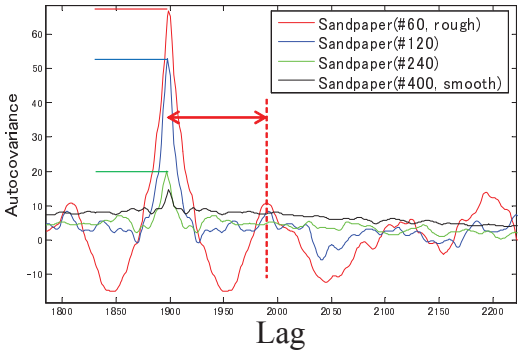

Figure 4.7 Zoomed autocovariance of friction (Sandpaper).

Feature values from the roughness

The results of the extracted feature values from the experiments are shown in Figure 4.9 and Figure 4.10. These results include one training data set and two test data sets. It seems that each surface is able to be distinguished although there are overlapping areas in these figures.

Feature values from the friction force

The results of the extracted feature values from the experiments are shown in Figure 4.11. These results include one training data set and two test data sets. It also seems that each surface is able to distinguish although there are overlapping areas in these figures.

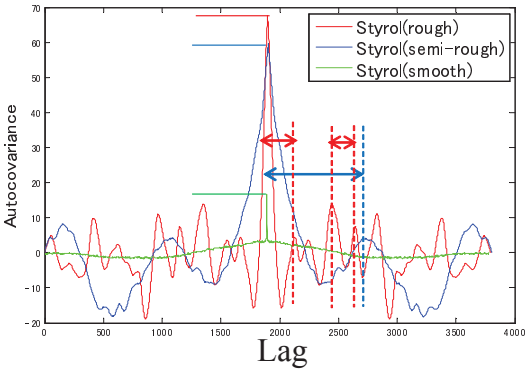

Figure 4.8 Zoomed autocovariance of friction (Styrol).

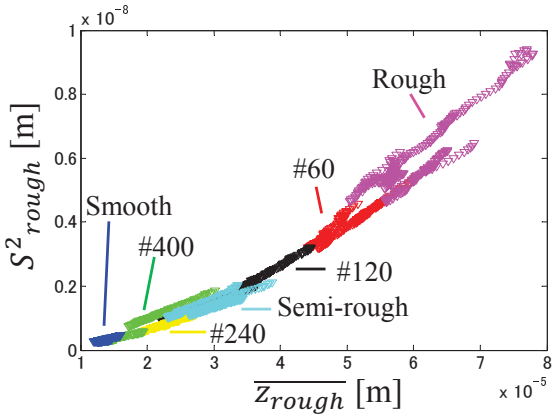

Figure 4.9 Average and sample variance of roughness.

4.3 Surface Recognition by SOM

Training

Results of the SOM model after learning are shown in Figure 4.12. Figure 4.12 is also called the topographic map. The SOM map represents the topology between nodes for each feature value. Therefore, the SOM map is used for some analyses. First, discrimination of the dominant feature value is possible. For example, feature values, whose SOM map changes smoothly and has clear map pattern, can be recognized as dominant feature values. Second, a correlation between one feature value and another feature value can be found. For example, there is a positive correlation

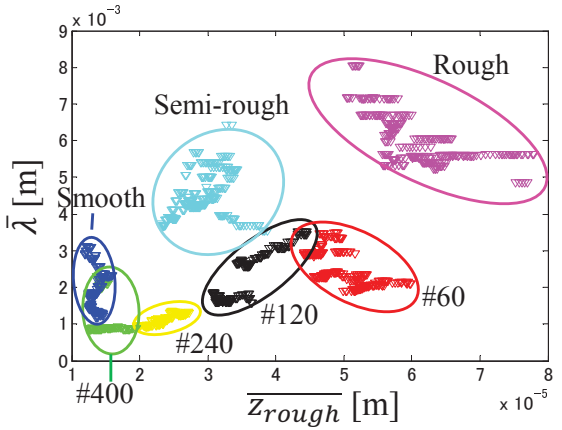

Figure 4.10 Average roughness and average wavelength.

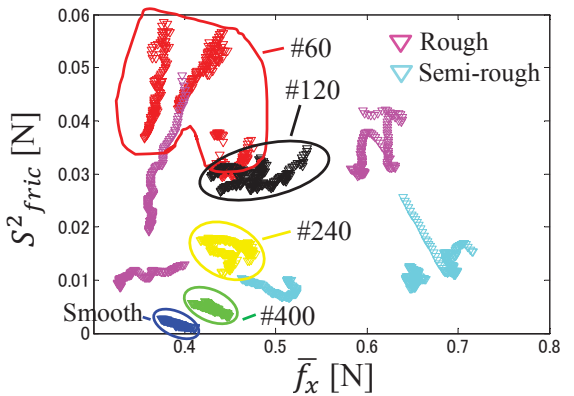

Figure 4.11 Average and sample variance of friction.

between feature 1 and feature 2 because they have a similar SOM map. Figure 4.9 also represents the positive correlation between feature 1 and feature 2.

Data density histogram of the training data using learned SOM model is shown in Figure 4.13 to check the validity of the SOM model. The data density histogram indicates the frequency of becoming "winner" nodes when comparing learned SOM models and feature vectors from training data. Winner nodes were decided by calculating Eq. (2.27). From Figure 4.13, all surfaces were classified with no overlapping.

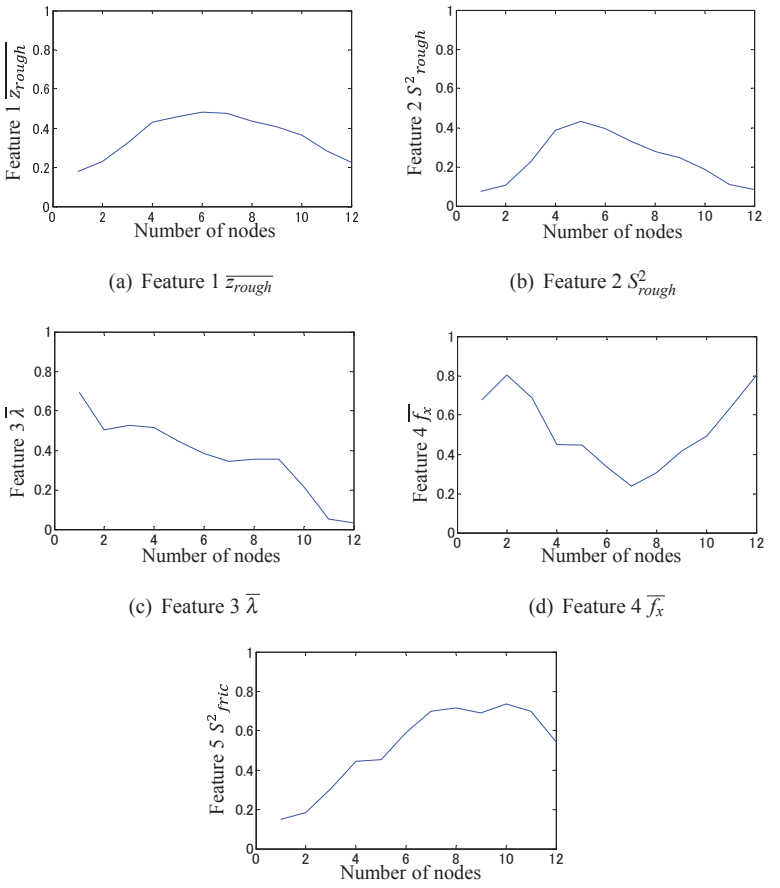

(a) Feature 1 $\overline{z_{rough}}$

(b) Feature 2 S^2_{rough}

(c) Feature 3 $\overline{\lambda}$

(d) Feature 4 $\overline{f_x}$

(e) Feature 5 S^2_{fric}

Figure 4.12 SOM model (Topographic map) after learning.

Surface recognition experiment

Figure 4.14 shows the recognition results using the SOM model shown in Figure 4.12. Recognition was started after $x = 0.005$ m. Surface 1, surface 3, surface 5 and surface 7 were recognized correctly at all position. In this study, however, the SOM model is changed every simulation due to the randomness of the initial reference vector. Therefore, surface recognition was conducted 10 times with same training data. Figure 4.15 shows the average recognition rate.

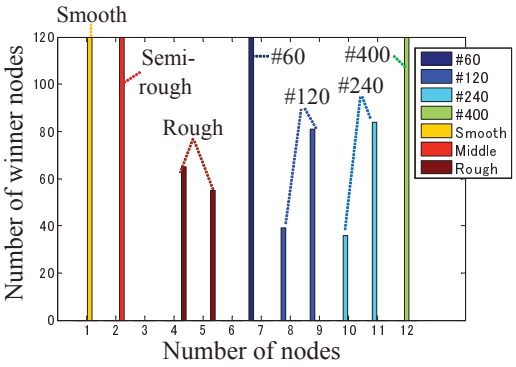

Figure 4.13 Data density histogram of training data using learned SOM model.

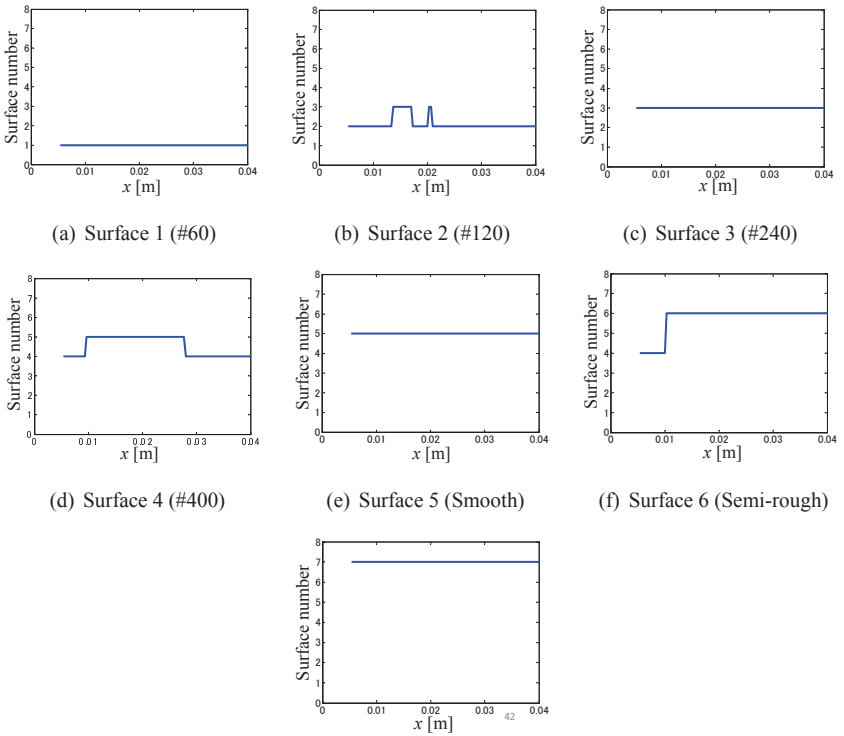

(a) Surface 1 (#60) (b) Surface 2 (#120) (c) Surface 3 (#240)

(d) Surface 4 (#400) (e) Surface 5 (Smooth) (f) Surface 6 (Semi-rough)

(g) Surface 7 (Rough)

Figure 4.14 Surface recognition results using SOM model shown in Figure 4.12.

Recognition results (%)

Experimental surface	1	2	3	4	5	6	7
1	100	0	0	0	0	0	0
2	0	78	22	0	0	0	0
3	0	6	94	0	0	0	0
4	0	0	0	46	49	5	0
5	0	0	0	0	96	4	0
6	0	0	0	7	0	93	0
7	0	0	0	0	0	0	100

Figure 4.15 Average recognition rate.

5

Discussion

5.1 Analysis of roughness and friction force

Section 4.1 shows the analysis results using autocovariance. There are two important points from this analysis.

First point is the maximum autocovariances. In Figure 4.2, 4 sandpapers can be distinguished by maximum autocovariances. Rougher sandpaper has bigger maximum autocovariance. In Figure 4.9 and Figure 4.10, the rougher surface exhibits larger average roughness. For these reasons, the maximum autocovariance is strongly related with average roughness. In other words, average roughness is one of the suitable feature value for surface recognition.

Second, the distance between maxima is also an important feature. In Figure 4.5, the sandpaper #120 and semi-rough surface have almost same autocovariances. However, the distance between maxima is different. Semi-rough styrol surface has bigger distance between maxima than #120. In Figure 4.10, semi-rough styrol surface has bigger average wavelength than #120. For these reasons, the distance between maxima is strongly related with average wavelength. In other words, the average wavelength is one of the suitable feature values for surface recognition.

5.2 Haptic Information Acquisition

Feature values were calculated from the roughness and the friction force in this paper.

From Figure 4.9, Figure 4.10 and Figure 4.11, all surfaces seem to be distinguished by using all feature values. However, there were data overlapping in some areas. Data overlapping mainly occurred between the smooth styrol and the sandpaper 400 surfaces of the roughness information. The reason is the thinness of the pen. In this paper, the pen was attached to the tip of the robot and the rubbing motion was conducted. Therefore, a resolution of the roughness depends on the thinness of the pen. Higher resolution of the roughness can be achieved by using thinner pen. However, thinness of the pen also affects to the friction. A thinner pen results in the

unreliable friction data. For these reasons, feature values used for decisions depend on the TCP probing tool of the robot.

5.3 Surface Recognition by SOM

From Figure 4.14 and Figure 4.15, recognition rate was high for most of the surfaces. Therefore, the validity of the proposed method was verified. However, recognition errors happened for some surfaces. These errors happened from some reasons.

First, randomness of the initial values of reference vector deteriorated the performance. Recognition rates can be improved by changing the initial values of reference vector. Second, the effect of SOM parameters shown in Table 3.3 has not been discussed or investigated in this paper. For example, it is possible to improve the performance by increasing the number of nodes s although the computation time is increased. Surface 4 (#400) and surface 5 (Smooth styrol) has similar feature values as shown in Figure 4.9, Figure 4.10 and Figure 4.11. Therefore, resolution of the haptic information acquisition system needs to be improved to distinguish surface 4 and surface 5 correctly.

6

Conclusion

In this paper, a new surface recognition method based on haptic information using SOM was proposed.

In the sensing part, roughness and friction force information were recorded by a haptic robot without a force sensors at the tip of the robot. Observers of type DOB and RFOB were applied to the Omega 7 robot. As a result, robust position control and reaction force estimation were achieved so that accurate roughness and friction could be estimated from the measurements. Feature values were calculated from the estimated roughness and friction force. From the results of the analysis using autocovariance as described and shown in Section 4.1, roughness and friction force have important characteristics to distinguish surfaces. From the results of the calculated feature values shown in Section 4.2, the validity of the feature values was verified. In addition to that, the limitation of the surface recognition method was shown. The resolution of the roughness and friction force depend on the probe. Users need to change the probe with respect to the surface recognition situation.

In the recognition part, Self-organizing map (SOM) was used. SOM is able to summarize high dimensional data to low dimension with preserving topological properties of data. Therefore, it is suitable to distinguish surfaces from some feature values. The SOM model was learned by using training data including calculated feature values. Surfaces were recognized using learned SOM model and test data. The validity of the proposed method was confirmed by experiments. Developing SOM such as changing initial values of reference vector and finding optimum SOM parameters are the future works to increase the recognition rate.

Bibliography

Boissieu, F. de, C. Godin, B. Guilhamat, D. David, C. Servière, and D. Baudois (2009). "Tactile texture recognition with a 3-axial force MEMS integrated artificial finger". In: *Robotics: Science and Systems V, University of Washington, June 28 - July 1, 2009, Seattle, USA*. URL: http://www.roboticsproceedings.org/rss05/p7.html [Accessed: 2014-09-11].

Brugger, D., M. Bogdan, and W. Rosenstiel (2008). "Automatic cluster detection in Kohonen's SOM". *Neural Networks, IEEE Transactions on* **19**:3, pp. 442–459. ISSN: 1045-9227. DOI: 10.1109/TNN.2007.909556.

Chacon-Murguia, M. and S. Gonzalez-Duarte (2012). "An adaptive neural-fuzzy approach for object detection in dynamic backgrounds for surveillance systems". *Industrial Electronics, IEEE Transactions on* **59**:8, pp. 3286–3298. ISSN: 0278-0046. DOI: 10.1109/TIE.2011.2106093.

Chen, C.-M., C.-C. Chen, and C.-C. Chen (2006). "A comparison of texture features based on SVM and SOM". In: *Pattern Recognition, 2006. ICPR 2006. 18th International Conference on*. Vol. 2, pp. 630–633. DOI: 10.1109/ICPR.2006.51.

Chow, T. W. S. and M. K. M. Rahman (2009). "Multilayer som with tree-structured data for efficient document retrieval and plagiarism detection". *Neural Networks, IEEE Transactions on* **20**:9, pp. 1385–1402. ISSN: 1045-9227. DOI: 10.1109/TNN.2009.2023394.

De Donno, A, F. Nageotte, P. Zanne, L. Zorn, and M. de Mathelin (2013). "Master/slave control of flexible instruments for minimally invasive surgery". In: *Intelligent Robots and Systems (IROS), IEEE/RSJ International Conference on, Nov. 3-8, 2013, Tokyo, Japan*, pp. 483–489. DOI: 10.1109/IROS.2013.6696395.

Ferre, M., I. Galiana, R. Wirz, and N. Tuttle (2011). "Haptic device for capturing and simulating hand manipulation rehabilitation". *Mechatronics, IEEE/ASME Transactions on* **16**:5, pp. 808–815. ISSN: 1083-4435. DOI: 10.1109/TMECH.2011.2159807.

From, P. J., J. H. Cho, A. Robertsson, T. Nakano, M. Ghazaei, and R. Johansson (2014). "Hybrid stiff/compliant workspace control for robotized minimally invasive surgery". In: *Biomedical Robotics and Biomechatronics (2014 5th IEEE RAS EMBS International Conference on*, pp. 345–351. DOI: 10.1109/BIOROB.2014.6913800.

Hosoda K. Tada, Y. and M. Asada (2006). "Anthropomorphic robotic soft fingertip with randomly distributed receptors". *Robot. Autom. Syst.* **54**:2, pp. 104–109. ISSN: 1045-9227. DOI: 10.1109/TNN.2007.909556.

Jain, A., R. P. W. Duin, and J. Mao (2000). "Statistical pattern recognition: a review". *Pattern Analysis and Machine Intelligence, IEEE Transactions on* **22**:1, pp. 4–37. ISSN: 0162-8828. DOI: 10.1109/34.824819.

Katsura, S., Y. Matsumoto, and K. Ohnishi (2007). "Modeling of force sensing and validation of disturbance observer for force control". *Industrial Electronics, IEEE Transactions on* **54**:1, pp. 530–538. ISSN: 0278-0046. DOI: 10.1109/TIE.2006.885459.

Kohonen, T. (2001). "Self-organizing maps". *ser. Information Sciences, 3rd ed. New York: Springer-Verlag*. ISSN: 0162-8828. DOI: 10.1109/34.824819.

Mizoguchi, T., T. Nozaki, and K. Ohnishi (2014). "Stiffness transmission of scaling bilateral control system by gyrator element integration". *Industrial Electronics, IEEE Transactions on* **61**:2, pp. 1033–1043. ISSN: 0278-0046. DOI: 10.1109/TIE.2013.2264787.

Motooka, W., T. Nozaki, T. Mizoguchi, K. Sugawara, F. Mitome, K. Okuda, M. Miyagaki, D. Yashiro, T. Yakoh, K. Ohnishi, Y. Morikawa, and N. Shimojima (2010). "Development of 16-dof telesurgical forceps master/slave robot with haptics". In: *IECON 2010 - 36th Annual Conference on IEEE Industrial Electronics Society*, pp. 2081–2086. DOI: 10.1109/IECON.2010.5675353.

Murakami, T., F. Yu, and K. Ohnishi (1993). "Torque sensorless control in multidegree-of-freedom manipulator". *IEEE Transactions on Industrial Electronics* **40**:2, pp. 259–265. ISSN: 0278-0046. DOI: 10.1109/41.222648.

Najmaei, N. and M. Kermani (2011). "Applications of artificial intelligence in safe human robot interactions". *Systems, Man, and Cybernetics, Part B: Cybernetics, IEEE Transactions on* **41**:2, pp. 448–459. ISSN: 1083-4419. DOI: 10.1109/TSMCB.2010.2058103.

Nozaki, T., T. Mizoguchi, Y. Saito, D. Yashiro, and K. Ohnishi (2013). "Recognition of grasping motion based on modal space haptic information using DP pattern-matching algorithm". *Industrial Informatics, IEEE Transactions on* **9**:4, pp. 2043–2051. ISSN: 1551-3203. DOI: 10.1109/TII.2012.2232934.

Nozaki, T., T. Mizoguchi, and K. Ohnishi (2014). "Decoupling strategy for position and force control based on modal space disturbance observer". *Industrial Electronics, IEEE Transactions on* **61**:2, pp. 1022–1032. ISSN: 0278-0046. DOI: 10.1109/TIE.2013.2264788.

Ohnishi, K., M. Shibata, and T. Murakami (1996). “Motion control for advanced mechatronics”. *IEEE/ASME Transactions on Mechatronics* **1**:1, pp. 56–67. ISSN: 1083-4435. DOI: 10.1109/3516.491410.

Romano, J. and K. Kuchenbecker (2012). “Creating realistic virtual textures from contact acceleration data”. *Haptics, IEEE Transactions on* **5**:2, pp. 109–119. ISSN: 1939-1412. DOI: 10.1109/TOH.2011.38.

Sinapov, J., V. Sukhoy, R. Sahai, and A. Stoytchev (2011). “Vibrotactile recognition and categorization of surfaces by a humanoid robot”. *Robotics, IEEE Transactions on* **27**:3, pp. 488–497. ISSN: 1552-3098. DOI: 10.1109/TRO.2011.2127130.

Watabe, T. and S Katsura (2011). “Recognition and classification of road condition on the basis of friction force by using a mobile robot”. *The transactions of the Institute of Electrical Engineers of Japan. D, A publication of Industry Applications Society* **131**:3, pp. 357–363. ISSN: 09136339. DOI: 10.1541/ieejias.131.357. URL: http://ci.nii.ac.jp/naid/10027805102/.

Zeng, T., B. Lemaire-Semail, F. Giraud, and M. Amberg (2013). “Contribution of slip cue to curvature perception through active and dynamic touch”. *Haptics, IEEE Transactions on* **6**:4, pp. 408–416. ISSN: 1939-1412. DOI: 10.1109/TOH.2013.21.

Lund University
Department of Automatic Control
Box 118
SE-221 00 Lund Sweden

Document name
MASTER´S THESIS

Date of issue
December 2014

Document Number
ISRN LUTFD2/TFRT--5957--SE

Author(s)
Tomohiro Nakano

Supervisor
Mahdi Ghazaei, Dept. of Automatic Control, Lund University, Sweden
Anders Robertsson, Dept. of Automatic Control, Lund University, Sweden
Rolf Johansson, Dept. of Automatic Control, Lund University, Sweden (examiner)

Sponsoring organization

Title and subtitle

Recognition of Surfaces Based on Haptic Information

Abstract

The main topic and focus in this thesis are surface recognition.

In the sensing part, the surface information is collected as feature values. There are research approaches which focus on sensing surface tactile information by using sensors with robots. However, there are some disadvantages of using sensors. From that reason, this thesis proposes getting haptic surface information without sensors at the tip of robots. To this purpose, a disturbance observer is implemented to achieve the robust acceleration control and a reaction force observer is implemented to estimate the friction force along surfaces.

In the recognition part, a pattern recognition method needs to be applied for surface recognition. There are some pattern recognition methods, where selforganizing maps (SOM) is one of the solutions and has been investigated. SOM is able to summarize high-dimensional data to low dimension with preserving the topological properties of data. SOM is also suitable for multi-class recognition. Therefore, a surface recognition using SOM is proposed in this thesis. Multi-class surface recognition is achieved by the proposed method.

The validity of the proposed method was confirmed through 7 surface recognition experiments. The recognition rate was over 90% for 5 of 7 surfaces in the time domain.

Keywords

Classification system and/or index terms (if any)

Supplementary bibliographical information

ISSN and key title
0280-5316

ISBN

Language
English

Number of pages
1-43

Recipient's notes

Security classification